frontiers in Bioengineering and Biotechnology

ORIGINAL RESEARCH
published: 10 December 2021
doi: 10.3389/fbioe.2021.767717

A Label-Free Electrochemical Immunosensor for CEA Detection on a Novel Signal Amplification Platform of Cu_2S/Pd/CuO Nanocomposites

Linlin Cao[1,2], *Wen Zhang*[2], *Sumei Lu*[1,3], *Chengjie Guo*[2], *Peijun Wang*[1], *Dantong Zhang*[3] *and Wanshan Ma*[1,3]*

[1]Department of Laboratory Medicine, Shandong Provincial Qianfoshan Hospital, Shandong University, Jinan, China, [2]Department of Clinical Laboratory, Zibo Central Hospital, Shandong University, Zibo, China, [3]Department of Laboratory Medicine, The First Affiliated Hospital of Shandong First Medical University, Jinan, China

Carcinoembryonic antigen (CEA) is regarded as one of the crucial tumor markers for colorectal cancer. In this study, we developed the snowflake Cu_2S/Pd/CuO nanocomposite to construct an original label-free electrochemical immunosensor for the ultrasensitive detection of CEA levels. The nanocomposite of cuprous sulfide (Cu_2S) with Pd nanoparticles (Pd NPs) was synthesized through an *in situ* formation of Pd NPs on the Cu_2S. Cuprous sulfide (Cu_2S) and CuO can not only be used as a carrier to increase the reaction area but also catalyze the substrate to generate current signal. Palladium nanoparticles (Pd NPs) have excellent catalytic properties and good biocompatibility, as well as the ability of excellent electron transfer. The immunosensor was designed using 5 mmol/L H_2O_2 as the active substrate by optimizing the conditions with a detection range from 100 fg/ml to 100 ng/ml and a minimum detection limit of 33.11 fg/ml. The human serum was detected by electrochemical immunoassay, and the results were consistent with those of the commercial electrochemical immunosensor. Therefore, the electrochemical immunosensor can be used for the detection of human serum samples and have potential value for clinical application.

Keywords: carcinoembryonic antigen, Cu_2S/Pd/CuO, immunosensor, colorectal cancer, label-free

OPEN ACCESS

Edited by:
Chaker Tlili,
Chongqing Institute of Green and Intelligent Technology (CAS), China

Reviewed by:
Nan-Fu Chiu,
National Taiwan Normal University, Taiwan
Niroj Kumar Sethy,
Defence Institute of Physiology and Allied Sciences (DRDO), India

***Correspondence:**
Wanshan Ma
mwsqianyi@163.com

Specialty section:
This article was submitted to Biosensors and Biomolecular Electronics, a section of the journal Frontiers in Bioengineering and Biotechnology

Received: *31 August 2021*
Accepted: *15 November 2021*
Published: *10 December 2021*

Citation:
Cao L, Zhang W, Lu S, Guo C, Wang P, Zhang D and Ma W (2021) A Label-Free Electrochemical Immunosensor for CEA Detection on a Novel Signal Amplification Platform of Cu_2S/Pd/CuO Nanocomposites. Front. Bioeng. Biotechnol. 9:767717. doi: 10.3389/fbioe.2021.767717

INTRODUCTION

Colorectal cancer (CRC) is one of the most frequent malignancies worldwide and is correlated with high mortality (Dekker et al., 2019). According to the latest statistics of the 2020 Global Cancer Statistics Report, there were 1,880,725 new cases of CRC. Colorectal cancer morbidity ranks third among malignancies, but second in terms of mortality (Sung et al., 2021). Carcinoembryonic antigen (CEA) is used as an important indicator for the diagnosis, treatment, recurrence, and metastasis of CRC (Konishi et al., 2018; Odeny et al., 2020). Additionally, CEA was also associated with other tumors, such as lung cancer (Grunnet and Sorensen, 2012), breast cancer (Tang et al., 2016), and pancreatic cancer (Xing et al., 2018). Therefore, it is essential to establish a rapid, sensitive, and reliable method for detecting CEA.

Currently, several assays have been applied to detect tumor markers in clinical practice, including enzyme-linked immunosorbent assay (ELISA) (Overholt et al., 2016; Zhang et al., 2019), electrochemiluminescence immunoassay (ECLI) (Wei et al., 2017; Nie et al., 2018),

electrochemical immunosensor (Yan et al., 2019; Xiang et al., 2020; Biswas et al., 2021; Jian et al., 2021), and radioimmunoassay (Poncelet et al., 2010; Kawamoto et al., 2019). Electrochemical immunosensors are biosensing devices that convert biochemical reactions into electrical signals based on the combination of highly sensitive sensing technology and specific immune reactions to study the reaction kinetics of antigens and corresponding antibodies. They have the advantages of high specificity and sensitivity, rapidity, low cost, and simple operation (Cho et al., 2018; Felix and Angnes, 2018). Particularly, label-free immunosensors directly detect the signal changes of the antigen–antibody complex, which greatly simplifies the sensor preparation and operation and does not require secondary antibody markers (Filik and Avan, 2019; Tan et al., 2020; Rahmati et al., 2021).

Nanomaterials, such as graphene oxide, metal nanoparticles, and metal–organic frameworks (MOFs), are often used as a means of signal amplification to heighten the sensitivity of sensors because of their high specific surface area, prominent electron transfer ability, and excellent biocompatibility (Song et al., 2016; Farka et al., 2017). Among them, metal nanomaterials (Chen et al., 2021; Simsek and Wongkaew, 2021) have attracted strong attention because of their stronger electrical conductivity, excellent catalysis, larger specific surface area, and convenient control. Palladium nanoparticles (Pd NPs) have efficient catalytic activity toward hydrogen peroxide substrates (Edwards et al., 2014; Trujillo et al., 2021) and are excellent materials for the construction of immunosensors (Han et al., 2020). However, when Pd NPs are exposed to a relatively harsh electrochemical environment, their stability worsens, resulting in the dissolution and migration of surface Pd atoms, which leads to the agglomeration of nanoparticles and the reduction of the surface area (Gao et al., 2019; Ma et al., 2020). Therefore, the noble metal materials of Pd are usually dispersed on the carrier to obtain nanocomposites with better biocompatibility, higher electrical conductivity, and more excellent catalytic performance.

In recent years, many researchers have focused on using semiconductor materials as carriers of noble metals to improve their catalytic performance, including metal oxides, MoS_2, and MOFs (Yang et al., 2017; Feng et al., 2018; Yusuf et al., 2021). The snowflake cuprous sulfide (Cu_2S), which has an exceptionally high surface area, is considered to be a potential support material to load Pd NPs. Herein, Cu_2S/Pd synthesized by *in situ* growth exhibiting satisfactory stability showed good catalytic performance and catalysis for hydrogen peroxide (H_2O_2) reduction (Zhang et al., 2018; Gao et al., 2020). Interestingly, we found that when Cu_2S was partly oxidized to CuO, the resulted Cu_2S/Pd/CuO nanocomposite possessed a more excellent catalytic performance, which could be a preferred signal amplification platform for the fabrication of immunosensors.

In this study, a novel composite material of Cu_2S/Pd/CuO was synthesized and used to construct a label-free electrochemical immunosensor for CEA sensing, achieving high sensitivity, a wide detection range, and a low detection limit, and was validated in the analysis of human serum samples. Therefore, the proposed immunosensor has great potential for clinical application.

MATERIALS AND METHODS

Reagents and Equipments

Ethylenediamine (EDA, CAS no. 107-15-3), $CuCl_2$ $2H_2O$ (CAS no. 10125-13-0), $(NH_2)_2CS$ (CAS no. 62-56-6), and Na_2PdCl_4 (CAS no. 13820-53-6) were purchased from Macklin Biochemical Co., Ltd. (Shanghai, China). Bovine serum albumin (BSA) (CAS no. 9048-46-8; storage, 2–8C), CEA (L2C01001, 2023-12; 1 mg/ml, −20C), and CEA antibody (L1C00202, 2023-12; 1.9 mg/ml, −20C) were from Shanghai Lingchao Biological New Material Technology Co., Ltd. (Shanghai, China). Phosphate buffer solutions (PBS) were prepared with Na_2HPO_4 (CAS no. 7558-79-4) and KH_2PO_4 (CAS no. 7778-77-0). Human serum was obtained from Zibo Central Hospital. Ultrapure water (18.25 Ω) was made in the laboratory throughout the experiments. Hydrogen peroxide (H_2O_2, 30 wt%) was purchased from Shuangshuang Chemical Co., Ltd. (Yantai, China).

The electrochemical measurements were performed on the electrochemical workstation (China). Conventional three-electrode systems used in electrochemical measurement include glass carbon electrode (GCE), saturated calomel electrode, and platinum wire electrode. The Tecnai G2 F20 transmission electron microscope (Hillsboro, OR, USA) was used for transmission electron microscopy (TEM) image acquisition. The JEOL JSM-6700F microscope (Tokyo, Japan) was used to record the X-ray energy (EDX) spectrum. SEM images were taken using the FEI Quanta FEG250 Field Emission Environmental Scanning Electron Microscope (Hillsboro, OR, USA).

Preparation of Cu_2S

The material preparation of Cu_2S was consistent with that reported in the literature (Zhang et al., 2018), and the method of hydrothermal synthesis was adopted. Firstly, 1 mmol $CuCl_2$ $2H_2O$ was dissolved in 30 ml EDA and 3 mmol thiourea was added. Then, the mixture was stirred with a magnetic mixer for 2 h at room temperature. After stirring, the mixed solution was transferred into a 50-ml polytetrafluoroethylene (PTFE) lined autoclave and reacted at 80°C for 8 h. Finally, the centrifugal Cu_2S was washed with anhydrous ethanol and secondary deionized water and then dried in a freeze dryer for the next step.

Preparation of Cu_2S/Pd

Polyvinylpyrrolidone (PVP, 50 mg) and synthesized Cu_2S (7.2 mg) were added into 8 ml secondary deionized water. Then, 5 ml of 10 mmol/L Na_2PdCl_4 solution was added to the above solution. Subsequently, the mixture was stirred with a magnetic mixer for 20 min and washed with ethanol and secondary deionized water three times. Finally, the obtained black powdery Cu_2S/Pd was dried in vacuum.

Preparation of Cu_2S/Pd/CuO

The GCE (0.4 μm in diameter) was first polished with 0.05 μm aluminum oxide powder and then thoroughly rinsed with ultrapure deionized water to acquire a fresh and transparent surface. The oxidation peak of bare GCE is less than 100 mV with

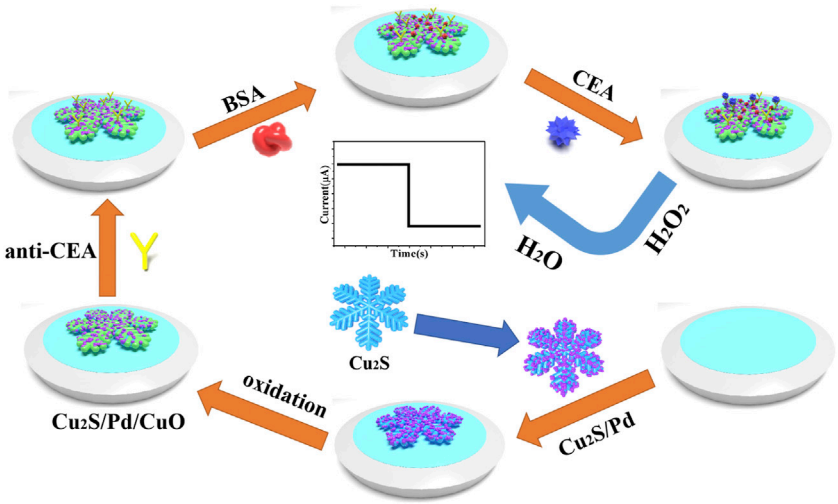

FIGURE 1 | Construction process of the electrochemical immunosensor for carcinoembryonic antigen (CEA) detection.

the reduction peak. The polished GCE was covered with deionized water to prevent oxidation, and then the electrode was blown dry with ear washers. Afterwards, the GCE electrode was modified with Cu_2S/Pd (6 μl, 2 mg/ml) and the three-electrode system was assembled. The electrode was placed into 10 ml PBS, and 40 μl H_2O_2 (5 M) was injected into PBS under the operation of chronoamperometry. Finally, the residual H_2O_2 on the surface of the working electrode was washed off with PBS and the modified electrode dried.

Preparation of Electrochemical Immunosensor

To illustrate the whole process of the experiment more clearly, **Figure 1** shows the layered self-assembly process of the immune sensor. The CEA antibody (anti-CEA, 6 μl, 2 mg/ml) was added to the surface of Cu_2S/Pd/CuO/GCE and incubated at 4C. After washing with PBS (pH 6.81), bovine serum albumin (BSA) solution (1 wt%, 3 μl) covered the anti-CEA/Cu_2S/Pd/CuO/GCE to block nonspecific active sites between the substrate nanocomposites and CEA. After 60 min of incubation, the BSA/anti-CEA/Cu_2S/Pd/CuO/GCE was washed with PBS (pH 6.81) and was added different concentration gradients of CEA (from 6 μl, 100 fg/ml to 100 ng/ml) for 60 min to optimize the reaction conditions between CEA and anti-CEA. Finally, the prepared working electrodes were washed with PBS (pH 6.81) and stored at 4°C.

Electrochemical Measurements

The electrochemical measurement was carried out using electrochemical workstation CHI760E. The immunosensor uses −0.4 V as the scanning potential to measure the current curve of the ampere. After the background current remained stable, H_2O_2 (5 M, 10 μl) was emptied into PBS (10 ml, pH 6.81), stirred with the magnetic stirrer, and the changes of the current response were recorded. The cyclic voltammetry (CV) test was carried out in K_3 [$Fe(CN)_6^{3-}$] solution (5 mM). Under the open circuit voltage of 0.196 V, electrochemical impedance spectroscopy (EIS) analysis was performed for the potassium ferricyanide solution, and a Nernst plot was drawn to record each fixed step. All the electrochemical measurement processes were conducted at room temperature.

RESULTS AND DISCUSSION

Characterization of Cu_2S, Cu_2S/Pd, and Cu_2S/Pd/CuO

Figure 2 shows the morphology of the prepared material. It can be found that the obtained Cu_2S is snowflake-shaped and has a flat symmetrical structure with six orientated petals radially extending from the central button; it has a diameter of 4–6 um based on the TEM image (**Figure 2A**). When Pd NPs wrapped around Cu_2S, they caused the Cu_2S/Pd to have an unclear boundary line and increased the specific surface area, as shown in **Figures 2B–D**. In **Figures 2E**, **F**, the successful preparation of Cu_2S/Pd/CuO nanocomposites was confirmed by TEM. The mapping spectra of Cu, S, Pd, and O (**Figures 3B–E**, respectively) clearly indicated that the distribution of the four elements was relatively uniform, specifying that the material is well constructed. At the same time, the EDX spectra (**Figure 3F**) confirmed that the composite material contained the Cu, S, Pd, and O elements.

Electrochemical Characterization

EIS can be used to compare the electrical conductivity of different materials (Strong et al., 2021). In this work, EIS was used to monitor the change of electron transfer resistance (R_{et}). The semicircle part represents the electron transfer limitation. The larger the semicircle diameter, the greater the R_{et}. Cu_2S (curve a) has poor electrical conductivity, which was obviously enhanced after palladium atoms were loaded and can be used as a substrate

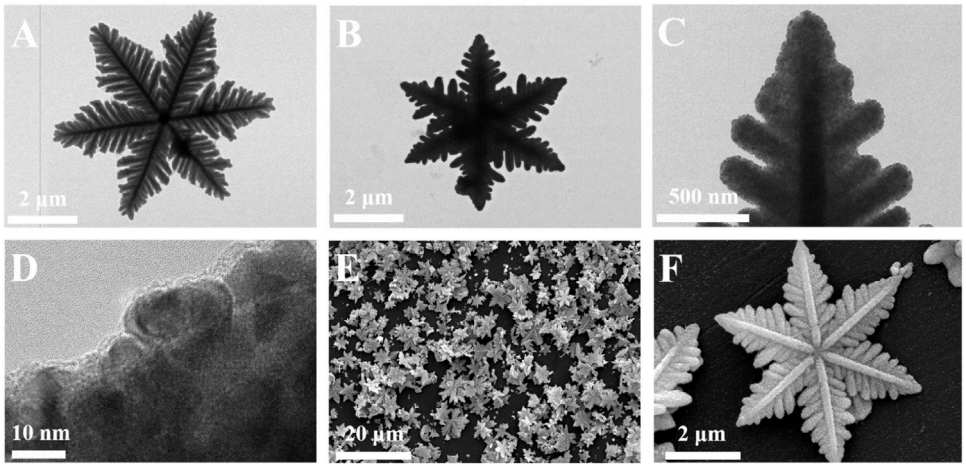

FIGURE 2 | (A–D) TEM images of Cu_2S **(A)** and Cu_2S/Pd **(B–D)**. **(E–F)** SEM images of Cu_2S/Pd/CuO.

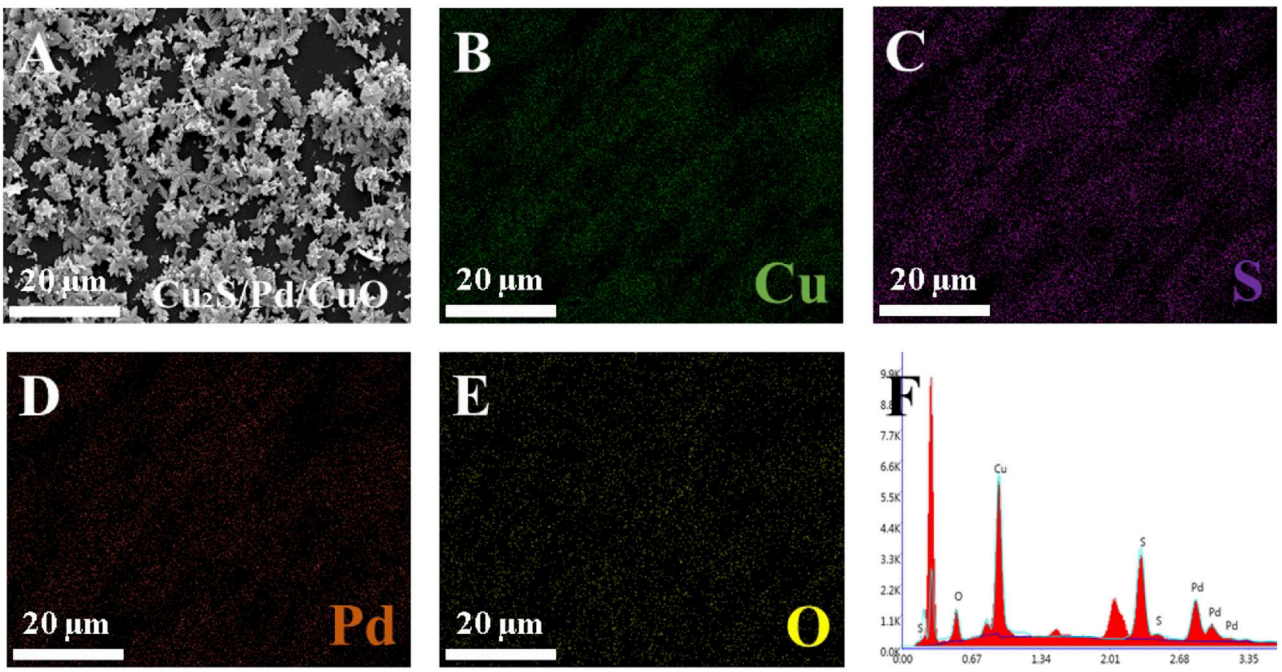

FIGURE 3 | Characterization of Cu_2S/Pd/CuO nanocomposites. **(A)** SEM image of Cu_2S/Pd/CuO. **(B–F)** Elemental mappings of Cu **(B)**, S **(C)**, Pd **(D)**, and O **(E)**. **(F)** X-ray energy (EDX) spectrum of Cu_2S/Pd/CuO.

material. The electrical conductivity of Cu_2S/Pd/CuO (curve c) was basically the same as that of Cu_2S/Pd (curve b), as shown in **Figure 4A** and **Supplementary Table S1**, indicating that Cu_2S/Pd/CuO has good electrical conductivity.

Immunosensors need to have good conductivity and catalysis, which are important for the collective effect of the various materials (Zheng et al., 2021). The sensitivity of the unlabeled immunosensor mainly depends on the reducibility of the constructed material to H_2O_2 (Yan et al., 2018). Chronoamperometry (*i–t*) can be used to compare the catalytic activities of different modified materials (Lee et al., 2018). As shown in **Figure 4B**, naked GCE has no catalytic activity for H_2O_2 (curve a). When Cu_2S was loaded onto the electrode, the catalytic signal increased slightly (curve b); the signal of Cu_2S/Pd (curve d) was greater than that of Cu_2S (curve b). This is due to the better catalytic performance of Pd NPs and the large specific surface area of snowflake-like materials, which can support more Pd NPs. Cu_2S generated Cu_2S/CuO (curve c) in the presence of hydrogen peroxide, and its catalytic activity was enhanced. It was further found in this experiment that the catalytic activity of Cu_2S/Pd/CuO

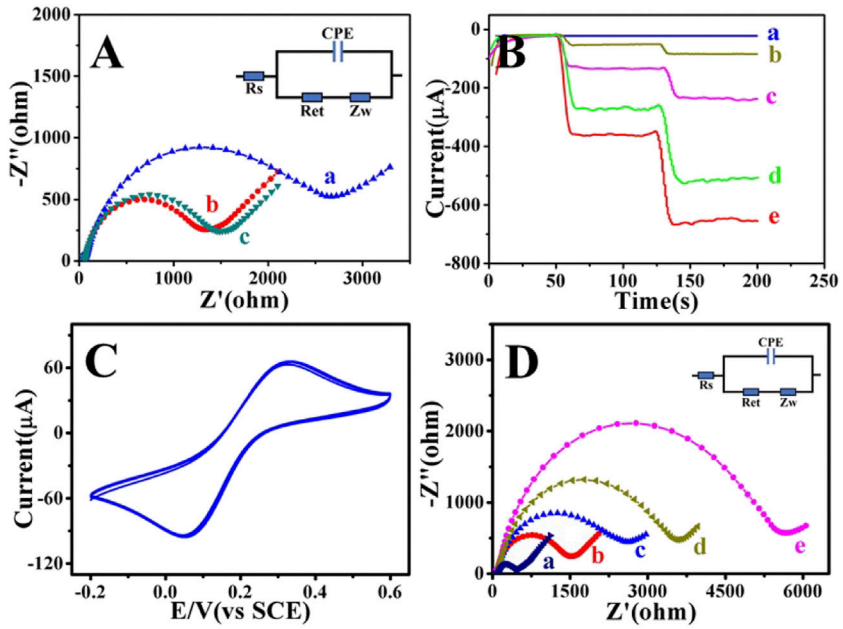

FIGURE 4 | Electrochemical characterization of Cu_2S/Pd/CuO nanocomposites. **(A)** Electrochemical impedance spectroscopy (EIS) of Cu_2S (*a*), Cu_2S/Pd (*b*), and Cu_2S/Pd/CuO (*c*). **(B)** Analysis of the *i–t* (current–time): glass carbon electrode (GCE) (*a*), Cu_2S (*b*), Cu_2S/CuO (*c*), Cu_2S/Pd (*d*), and Cu_2S/Pd/CuO (*e*). **(C)** Cyclic voltammetry (CV) diagram of Cu_2S/Pd/CuO-modified GCE. **(D)** EIS of GCE (*a*), Cu_2S/Pd/CuO/GCE (*b*), anti-CEA/Cu_2S/Pd/CuO/GCE (*c*), BSA/anti-CEA/Cu_2S/Pd/CuO/GCE (*d*), and CEA/BSA/anti-CEA/Cu_2S/Pd/CuO/GCE (*e*). *BSA*, bovine serum albumin; *CEA*, carcinoembryonic antigen.

(curve e) was higher than that of Cu_2S/Pd (curve d), and the current response was more stable. Therefore, the Cu_2S/Pd/CuO nanocomposite material was used as a signal-amplifying platform to construct a highly sensitive and unlabeled electrochemical immunosensor. After the modification of Cu_2S/Pd/CuO on the GCE, the peak current after multiple scanning, calculated by measuring the CV response, was basically unchanged, indicating that the prepared nanocomposite has good stability (**Figure 4C**). The successful construction of the sensor was verified by EIS detection of layers of modification (**Figure 4D** and **Supplementary Table S2**). Compared with the bare GCE (curve a), the resistance of the Cu_2S/Pd/CuO (curve b) electrode was higher. When anti-CEA (curve c), BSA (curve d), and CEA (curve e) were successively modified to the working electrode surface, the semicircle diameter of the electrical impedance spectra increased continuously, which was attributed to the partial inhibition of electron transfer by proteins (**Supplementary Table S2**), indicating that the electrochemical immunosensor was successfully modified.

Optimization of the Experimental Conditions

In order to obtain the best measurement results for the tumor markers, experimental conditions such as the substrate concentration of Cu_2S/Pd/CuO and the pH of PBS need to be optimized. The immunosensor was constructed based on a CEA concentration of 1 ng/ml in this study.

The pH value of PBS is important for the catalytic properties of the immunosensor because a strongly acidic or alkaline environment may inactivate antigens and antibodies, thus affecting the specificity of protein binding. When the pH of PBS changed from 5.91 to 6.81, the current signal began to increase to a peak. However, when the pH of PBS exceeded 6.81, the current response was reduced. Therefore, the maximum current signal was obtained at a pH of 6.81, which maintained good biological activity. Therefore, PBS with pH of 6.81 was selected as the best electrolyte for electrochemical measurements (**Figure 5A**). The concentration of Cu_2S/Pd/CuO is one of the most important parameters affecting the performance of the electrochemical immunosensor. The concentration of Cu_2S/Pd/CuO will have an impact on the electron transfer and the loading capacity of the anti-CEA. In order to obtain the best performance of the immunosensor, working electrodes with different concentrations of Cu_2S/Pd/CuO were used, and 10 μl (5.0 mM) H_2O_2 was injected into 10 ml PBS at pH 6.81. As shown in **Figure 5B**, the current response increased significantly with the increase of Cu_2S/Pd/CuO concentration from 0.5 to 2.0 mg/ml, and then decreased gradually with the increase of Cu_2S/Pd/CuO concentration from 2.0 to 3.0 mg/ml. Therefore, the optimal concentration for the immunosensor construction in this study was 2.0 mg/ml.

Performance Analysis of the Immunosensor

In this experiment, an electrochemical immunosensor with good conductivity and catalytic activity was prepared with the Cu_2S/Pd/CuO composite material. A series of CEA concentrations were measured by chronoamperometry. With the increase of CEA concentration, the current signal of the immune sensor decreased, indicating that the antigen impeded the electron transport (**Figure 6A**). In the range from 100 fg/ml to 100 ng/ml, the

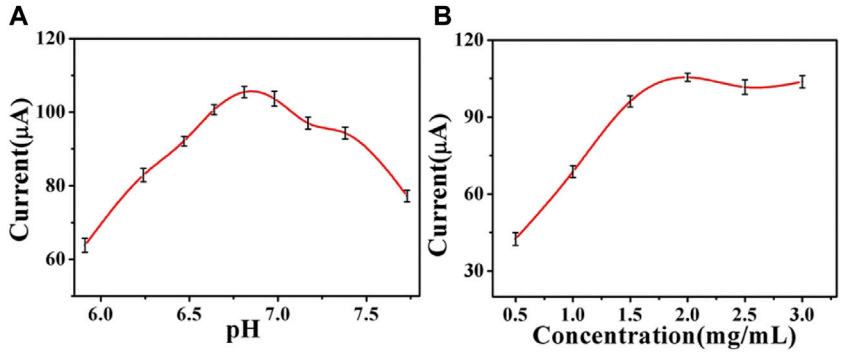

FIGURE 5 | Optimization of the experimental conditions of the pH value **(A)** and Cu_2S/Pd/CuO concentration **(B)**. Error bar = SD.

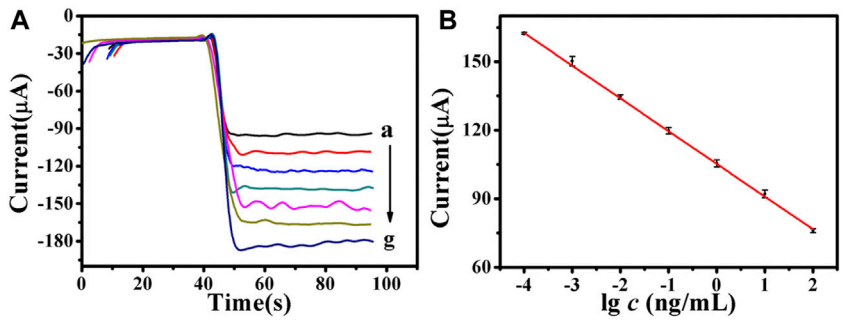

FIGURE 6 | (A) Amperometric response of the electrochemical immunosensor to different concentrations of carcinoembryonic antigen (CEA), from *a* to *g*: 100 fg/ml, 1 pg/ml, 10 pg/ml, 100 pg/ml, 1 ng/ml, 10 ng/ml, 100 ng/ml, respectively. **(B)** Calibration curves of the immunosensor to different concentrations of CEA. Error bar = SD.

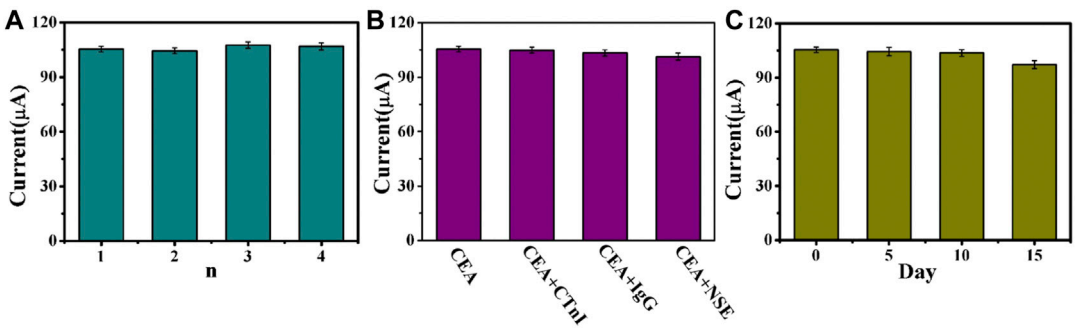

FIGURE 7 | (A) Current change response of the biosensor to five different electrodes treated in the same process (carcinoembryonic antigen, CEA = 1 ng/ml). **(B)** Current signals of the compound of interfering substances (20 ng/ml) and CEA (1 ng/ml). **(C)** Stability study of the CEA immunosensor (CEA = 1 ng/ml). Error bar = SD.

TABLE 1 | Detection of carcinoembryonic antigen (CEA) in human serum samples

CEA content in serum (ng/ml)	Addition content (ng/ml)	Detection value (ng/ml)	Recovery (%)
2.58	1.00	3.86	108
	5.00	7.33	96.7
	10.0	12.0	95.5

linear regression equation of the CEA concentration to the value and current response was $Y = -14.34\lg C + 105.24$, and the correlation coefficient was 0.9997 (**Figure 6B**). The limit of detection (LOD) was 33.11 fg/ml (S/N = 3).

Compared with other reported CEA results of the immunosensor (**Supplementary Table S3**), the immunosensor in this study showed a comparable linear range (from 100 fg/ml to 100 ng/ml) and an improved LOD (33.11 fg/ml). The reasons for the low detection limit of the prepared immunosensor were as follows: firstly, Cu_2S/Pd/CuO has good biocompatibility, which ensures antigen activity and can effectively fix antibodies. Secondly, Cu_2S/Pd/CuO can provide a wider detection range as a multi-signal amplification platform. Finally, Cu_2S/Pd/CuO has good electron transfer performance, which benefits improving the sensitivity of the electrochemical immunosensor.

After the electrochemical immunosensor was prepared, its performance needs to be verified, such as its repeatability, selectivity, and stability. These are important parameters for the evaluation of clinical application methods. Firstly, five immunosensors were prepared with the same concentration of CEA by chronoamperometry to detect the current signal; the repeatability of the electrochemical immunosensor was then studied. The relative standard deviation (RSD) of the electrode was calculated as 1.15%, indicating that the immune sensor has good repeatability (**Figure 7A**). Secondly, the selectivity of the immunosensor was studied using troponin I (CTnI), immunoglobulin G (IgG), and neuron-specific enolase (NSE) as the interfering substances. As shown in **Figure 7B**, the RSD was less than 1.79%, indicating that the selectivity of the immunosensor is relatively reliable. Finally, the stability of the immunosensor was assessed by measuring the current response of the five working electrodes and storing them in a 4C refrigerator when not tested once a day for five consecutive days. After 15 days, the current signal obtained decreased from 100% to 92.1% (**Figure 7C**), showing good stability. The experimental results showed that the immunosensor has good reproducibility, selectivity, and stability and can be used for highly sensitive and quantitative detection of CEA.

Detection of CEA in Human Serum Samples

In order to evaluate the application potential and reliability of the immunosensor designed in this study, a standard recovery experiment and human serum sample test were conducted. The results showed that the recoveries were 95.5%–108%, as shown in **Table 1**. Compared with that of commercial electrochemiluminescence immunoassay (ECLIA), the relative error was 3.70%–5.89% (**Supplementary Table S4**), which proves the feasibility of the designed immunosensor. These results indicate that the constructed immunosensor has potential application value in clinical serum CEA detection.

CONCLUSION

We used Cu_2S/Pd/CuO as the signal amplification platform to successfully prepare an unlabeled immunosensor that can detect CEA quantitatively and sensitively. The Cu_2S/Pd/CuO sensing platform can effectively capture the substance to be measured, amplify the current signal, and improve the catalytic performance. The unlabeled immunosensor has good specificity, repeatability, and stability. At the same time, the detection limit of the electrochemical method is low and the linear range is wide, which meet the requirements of human serum sample detection. This strategy has important application value in the clinical diagnosis related to other molecular markers.

DATA AVAILABILITY STATEMENT

The original contributions presented in the study are included in the article/**Supplementary Material**. Further inquiries can be directed to the corresponding author.

ETHICS STATEMENT

The studies involving human participants were reviewed and approved by the Medical Ethics Expert Committee of Zibo Central Hospital. The patients/participants provided written informed consent to participate in this study.

AUTHOR CONTRIBUTIONS

LC collected the experimental data and wrote the manuscript. WZ, SL, and CG performed the device fabrication. PW and DZ performed data analysis. WM oversaw the project and reviewed the manuscript.

FUNDING

This study was funded by Shandong Provincial Major Engineering and Major Program For Replacing Old Growth Drivers With New One Presided over by Wanshan Ma in 2021; the Cultivation Fund of National Natural Science Foundation of China in Shandong Provincial Qianfoshan Hospital (No. QYPY2020NSFC1004, No. QYPY2021NSFC0804), and the Key Technology Research and Development Program of Shandong (No. 2017G006024).

ACKNOWLEDGMENTS

This study was supported by the Department of Laboratory Medicine of Shandong Provincial Qianfoshan Hospital and the Department of Clinical Laboratory of Zibo Central Hospital. The authors acknowledge the organizations for their support and help.

SUPPLEMENTARY MATERIAL

The Supplementary Material for this article can be found online at: https://www.frontiersin.org/articles/10.3389/fbioe.2021.767717/full#supplementary-material

REFERENCES

Biswas, S., Lan, Q., Xie, Y., Sun, X., and Wang, Y. (2021). Label-Free Electrochemical Immunosensor for Ultrasensitive Detection of Carbohydrate Antigen 125 Based on Antibody-Immobilized Biocompatible MOF-808/CNT. *ACS Appl. Mater. Inter.* 13 (2), 3295–3302. doi:10.1021/acsami.0c14946

Chen, X., Peng, M., Cai, X., Chen, Y., Jia, Z., Deng, Y., et al. (2021). Regulating Coordination Number in Atomically Dispersed Pt Species on Defect-Rich Graphene for N-Butane Dehydrogenation Reaction. *Nat. Commun.* 12 (1), 2664. doi:10.1038/s41467-021-22948-w

Cho, I.-H., Lee, J., Kim, J., Kang, M.-s., Paik, J., Ku, S., et al. (2018). Current Technologies of Electrochemical Immunosensors: Perspective on Signal Amplification. *Sensors* 18 (1), 207. doi:10.3390/s18010207

Dekker, E., Tanis, P. J., Vleugels, J. L. A., Kasi, P. M., and Wallace, M. B. (2019). Colorectal Cancer. *The Lancet* 394 (10207), 1467–1480. doi:10.1016/s0140-6736(19)32319-0

Edwards, J. K., Freakley, S. J., Carley, A. F., Kiely, C. J., and Hutchings, G. J. (2014). Strategies for Designing Supported Gold-Palladium Bimetallic Catalysts for the Direct Synthesis of Hydrogen Peroxide. *Acc. Chem. Res.* 47 (3), 845–854. doi:10.1021/ar400177c

Farka, Z., Juřík, T., Kovář, D., Trnková, L., and Skládal, P. (2017). Nanoparticle-Based Immunochemical Biosensors and Assays: Recent Advances and Challenges. *Chem. Rev.* 117 (15), 9973–10042. doi:10.1021/acs.chemrev.7b00037

Felix, F. S., and Angnes, L. (2018). Electrochemical Immunosensors - A Powerful Tool for Analytical Applications. *Biosens. Bioelectron.* 102, 470–478. doi:10.1016/j.bios.2017.11.029

Feng, J., Li, F., Li, X., Wang, Y., Fan, D., Du, B., et al. (2018). Label-free Photoelectrochemical Immunosensor for NT-proBNP Detection Based on La-CdS/3D ZnIn2S4/Au@ZnO Sensitization Structure. *Biosens. Bioelectron.* 117, 773–780. doi:10.1016/j.bios.2018.07.015

Filik, H., and Avan, A. A. (2019). Nanostructures for Nonlabeled and Labeled Electrochemical Immunosensors: Simultaneous Electrochemical Detection of Cancer Markers: A Review. *Talanta* 205, 120153. doi:10.1016/j.talanta.2019.120153

Gao, H., Zhai, C., Yuan, C., Liu, Z.-Q., and Zhu, M. (2020). Snowflake-like Cu2S as Visible-Light-Carrier for Boosting Pd Electrocatalytic Ethylene Glycol Oxidation under Visible Light Irradiation. *Electrochimica Acta* 330, 135214. doi:10.1016/j.electacta.2019.135214

Gao, Z., Li, Y., Zhang, C., Zhang, S., Li, F., Wang, P., et al. (2019). Label-free Electrochemical Immunosensor for Insulin Detection by High-Efficiency Synergy Strategy of Pd NPs@3D MoSx towards H2O2. *Biosens. Bioelectron.* 126, 108–114. doi:10.1016/j.bios.2018.10.017

Grunnet, M., and Sorensen, J. B. (2012). Carcinoembryonic Antigen (CEA) as Tumor Marker in Lung Cancer. *Lung Cancer* 76 (2), 138–143. doi:10.1016/j.lungcan.2011.11.012

Han, G.-H., Xiao, X., Hong, J., Lee, K.-J., Park, S., Ahn, J.-P., et al. (2020). Tailored Palladium-Platinum Nanoconcave Cubes as High Performance Catalysts for the Direct Synthesis of Hydrogen Peroxide. *ACS Appl. Mater. Inter.* 12 (5), 6328–6335. doi:10.1021/acsami.9b21558

Jian, L., Wang, X., Hao, L., Liu, Y., Yang, H., Zheng, X., et al. (2021). Electrochemiluminescence Immunosensor for Cytokeratin Fragment Antigen 21-1 Detection Using Electrochemically Mediated Atom Transfer Radical Polymerization. *Microchim Acta* 188 (4), 115. doi:10.1007/s00604-020-04677-x

Kawamoto, H., Hara, H., Araya, J., Ichikawa, A., Fujita, Y., Utsumi, H., et al. (2019). Prostaglandin E-Major Urinary Metabolite (PGE-MUM) as a Tumor Marker for Lung Adenocarcinoma. *Cancers* 11 (6), 768. doi:10.3390/cancers11060768

Konishi, T., Shimada, Y., Hsu, M., Tufts, L., Jimenez-Rodriguez, R., Cercek, A., et al. (2018). Association of Preoperative and Postoperative Serum Carcinoembryonic Antigen and Colon Cancer Outcome. *JAMA Oncol.* 4 (3), 309–315. doi:10.1001/jamaoncol.2017.4420

Lee, G.-Y., Park, J.-H., Chang, Y. W., Cho, S., Kang, M.-J., and Pyun, J.-C. (2018). Chronoamperometry-Based Redox Cycling for Application to Immunoassays. *ACS Sens.* 3 (1), 106–112. doi:10.1021/acssensors.7b00681

Ma, E., Wang, P., Yang, Q., Yu, H., Pei, F., Zheng, Y., et al. (2020). Electrochemical Immunosensors for Sensitive Detection of Neuron-specific Enolase Based on Small-Size Trimetallic Au@PdPt Nanocubes Functionalized on Ultrathin MnO2 Nanosheets as Signal Labels. *ACS Biomater. Sci. Eng.* 6 (3), 1418–1427. doi:10.1021/acsbiomaterials.9b01882

Nie, G., Wang, Y., Tang, Y., Zhao, D., and Guo, Q. (2018). A Graphene Quantum Dots Based Electrochemiluminescence Immunosensor for Carcinoembryonic Antigen Detection Using Poly(5-Formylindole)/reduced Graphene Oxide Nanocomposite. *Biosens. Bioelectron.* 101, 123–128. doi:10.1016/j.bios.2017.10.021

Odeny, T. A., Farha, N., Hildebrandand, H., Allen, J., Vazquez, W., Martinez, M., et al. (2020). Association between Primary Perioperative CEA Ratio, Tumor Site, and Overall Survival in Patients with Colorectal Cancer. *Jcm* 9 (12), 3848. doi:10.3390/jcm9123848

Overholt, B. F., Wheeler, D. J., Jordan, T., and Fritsche, H. A. (2016). CA11-19: a Tumor Marker for the Detection of Colorectal Cancer. *Gastrointest. Endosc.* 83 (3), 545–551. doi:10.1016/j.gie.2015.06.041

Poncelet, C., Fauvet, R., Yazbeck, C., Coutant, C., and Darai, E. (2010). Impact of Serum Tumor Marker Determination on the Management of Women with Borderline Ovarian Tumors: Multivariate Analysis of a French Multicentre Study. *Eur. J. Surg. Oncol. (Ejso)* 36 (11), 1066–1072. doi:10.1016/j.ejso.2010.07.004

Rahmati, Z., Roushani, M., Hosseini, H., and Choobin, H. (2021). Electrochemical Immunosensor with Cu2O Nanocube Coating for Detection of SARS-CoV-2 Spike Protein. *Microchim Acta* 188 (3), 105. doi:10.1007/s00604-021-04762-9

Simsek, M., and Wongkaew, N. (2021). Carbon Nanomaterial Hybrids via Laser Writing for High-Performance Non-enzymatic Electrochemical Sensors: a Critical Review. *Anal. Bioanal. Chem.* 413, 6079–6099. doi:10.1007/s00216-021-03382-9

Song, Y., Luo, Y., Zhu, C., Li, H., Du, D., and Lin, Y. (2016). Recent Advances in Electrochemical Biosensors Based on Graphene Two-Dimensional Nanomaterials. *Biosens. Bioelectron.* 76, 195–212. doi:10.1016/j.bios.2015.07.002

Strong, M. E., Richards, J. R., Torres, M., Beck, C. M., and La Belle, J. T. (2021). Faradaic Electrochemical Impedance Spectroscopy for Enhanced Analyte Detection in Diagnostics. *Biosens. Bioelectron.* 177, 112949. doi:10.1016/j.bios.2020.112949

Sung, H., Ferlay, J., Siegel, R. L., Laversanne, M., Soerjomataram, I., Jemal, A., et al. (2021). Global Cancer Statistics 2020: GLOBOCAN Estimates of Incidence and Mortality Worldwide for 36 Cancers in 185 Countries. *CA A. Cancer J. Clin.* 71, 209–249. doi:10.3322/caac.21660

Tan, Z., Cao, L., He, X., Dong, H., Liu, Q., Zhao, P., et al. (2020). A label-free immunosensor for the sensitive detection of hepatitis B e antigen based on PdCu tripod functionalized porous graphene nanoenzymes. *Bioelectrochemistry* 133, 107461. doi:10.1016/j.bioelechem.2020.107461

Tang, S., Zhou, F., Sun, Y., Wei, L., Zhu, S., Yang, R., et al. (2016). CEA in Breast Ductal Secretions as a Promising Biomarker for the Diagnosis of Breast Cancer: a Systematic Review and Meta-Analysis. *Breast Cancer* 23 (6), 813–819. doi:10.1007/s12282-016-0680-9

Trujillo, R. M., Barraza, D. E., Zamora, M. L., Cattani-Scholz, A., and Madrid, R. E. (2021). Nanostructures in Hydrogen Peroxide Sensing. *Sensors* 21 (6), 2204. doi:10.3390/s21062204

Wei, X., Li, Y.-b., Li, Y., Lin, B.-c., Shen, X.-M., Cui, R.-L., et al. (2017). Prediction of Lymph Node Metastases in Gastric Cancer by Serum APE1 Expression. *J. Cancer* 8 (8), 1492–1497. doi:10.7150/jca.18615

Xiang, W., Lv, Q., Shi, H., Xie, B., and Gao, L. (2020). Aptamer-based Biosensor for Detecting Carcinoembryonic Antigen. *Talanta* 214, 120716. doi:10.1016/j.talanta.2020.120716

Xing, H., Wang, J., Wang, Y., Tong, M., Hu, H., Huang, C., et al. (2018). Diagnostic Value of CA 19-9 and Carcinoembryonic Antigen for Pancreatic Cancer: A Meta-Analysis. *Gastroenterol. Res. Pract.* 2018, 1–9. doi:10.1155/2018/8704751

Yan, Q., Cao, L., Dong, H., Tan, Z., Hu, Y., Liu, Q., et al. (2019). Label-free Immunosensors Based on a Novel Multi-Amplification Signal Strategy of TiO2-NGO/Au@Pd Hetero-Nanostructures. *Biosens. Bioelectron.* 127, 174–180. doi:10.1016/j.bios.2018.12.038

Yan, Q., Yang, Y., Tan, Z., Liu, Q., Liu, H., Wang, P., et al. (2018). A Label-free Electrochemical Immunosensor Based on the Novel Signal Amplification System of AuPdCu Ternary Nanoparticles Functionalized Polymer Nanospheres. *Biosens. Bioelectron.* 103, 151–157. doi:10.1016/j.bios.2017.12.040

Yang, Q., Xu, Q., and Jiang, H.-L. (2017). Metal-organic Frameworks Meet Metal Nanoparticles: Synergistic Effect for Enhanced Catalysis. *Chem. Soc. Rev.* 46 (15), 4774–4808. doi:10.1039/c6cs00724d

Yusuf, M., Song, S., Park, S., and Park, K. H. (2021). Multifunctional Core-Shell Pd@Cu on MoS2 as a Visible Light-Harvesting Photocatalyst for Synthesis of Disulfide by S S Coupling. *Appl. Catal. A: Gen.* 613, 118025. doi:10.1016/j.apcata.2021.118025

Zhang, D., Li, W., Ma, Z., and Han, H. (2019). Improved ELISA for Tumor Marker Detection Using Electro-Readout-Mode Based on Label Triggered Degradation of Methylene Blue. *Biosens. Bioelectron.* 126, 800–805. doi:10.1016/j.bios.2018.11.038

Zhang, X., Guo, Y., Tian, J., Sun, B., Liang, Z., Xu, X., et al. (2018). Controllable Growth of MoS2 Nanosheets on Novel Cu2S Snowflakes with High Photocatalytic Activity. *Appl. Catal. B: Environ.* 232, 355–364. doi:10.1016/j.apcatb.2018.03.074

Zheng, Y., Li, J., Zhou, B., Ian, H., and Shao, H. (2021). Advanced Sensitivity Amplification Strategies for Voltammetric Immunosensors of Tumor Marker: State of the Art. *Biosens. Bioelectron.* 178, 113021. doi:10.1016/j.bios.2021.113021

Conflict of Interest: The authors declare that the research was conducted in the absence of any commercial or financial relationships that could be construed as a potential conflict of interest.